euspen's 26th International Conference & Exhibition, Krakow, PL, June 2026
www.euspen.eu

Lateral resolution enhancement of white light scanning interferometer

Min Seo Cho[1] and Ki-Nam Joo[1]

[1]*Department of Photonic engineering, Chosun University, Gwangju, Republic of Korea*

Corresponding Author: Knjoo@chosun.ac.kr

Abstract
Recently, semiconductor manufacturing technologies have been developed to achieve high integration in semiconductor processes. Various 3D surface measurement optical instruments are currently used in the industry, and structured illumination microscopy can reconstruct high resolution 2D surface of the specimen through the phase shifting of the pattern. Also, white light scanning interferometry can reconstruct the 3D surface of the specimen through scanning of the specimen by interference signal. In this investigation, we propose high resolution white light scanning interferometry which merges structured illumination microscopy and white light scanning interferometry.

Structured illumination microscopy, White light scanning interferometry, Structured illumination white-light scanning interferometry

1. Introduction

Recently, various semiconductor manufacturing technologies such as miniaturization and multi-chip package (MCP) have been developed to achieve high integration in semiconductor processes. In the miniaturization and MCP process of these semiconductors, 3D measurement and inspection technologies are essential elements for improving product performance and process stability. For the purpose, confocal scanning microscopes and interferometric microscopes [1-4] are currently applied to meet the demands required by industries. However, the conventional microscopes have fundamental limitations in obtaining high-resolution images due to the lateral resolution limit by the numerical aperture (NA) of the objective lens, which causes problems in obtaining accurate height values of 3D reconstruction results. In 3D surface profilers, furthermore, the lateral resolution limit is propagated to height measurement capability of the system, and the height measurement precision and accuracy can be significantly alleviated.

Meanwhile, structured illumination microscopy widely used in the biomedical fields can obtain the extended spatial frequency content from the image by applying multiple rotating phase-shifted sinusoidal patterns, and restores a high-resolution image that overcomes the diffraction limit through the entire spatial frequency domain obtained computationally from all images.

In this investigation, we propose high resolution white light scanning interferometry (HR-WLSI) that is a combination of white light scanning interferometry (WLSI) and structured illumination microscopy (SIM), which can overcome the lateral resolution limit through various angle rotation and phase shifting of sinusoidal illumination pattern [5-7]. A digital micromirror device (DMD) is used to generate sinusoidal illumination patterns of various rotation angles, and a Mirau type objective lens is used to acquire interference signals. To experimentally verify the system performance, various step height standard specimens were measured.

2. The principle of lateral resolution enhancement of white light scanning interferometry

2.1 HR-WLSI

Figure 1 shows an optical configuration of HR-WLSI, which is a combination of WLSI and SIM. In HR-WLSI, a DMD was used for generating the sinusoidal pattern for the illumination, of which the pattern was rotated and phase shifted. The illumination pattern generated by DMD passes through the focal lens and objective lens, and it is imaged on the specimen. At this time, the objective lens is a Mirau type objective lens, and an interference fringe is generated through an internal reference mirror and plate beam splitter. After, an image is acquired from a camera through a tube lens.

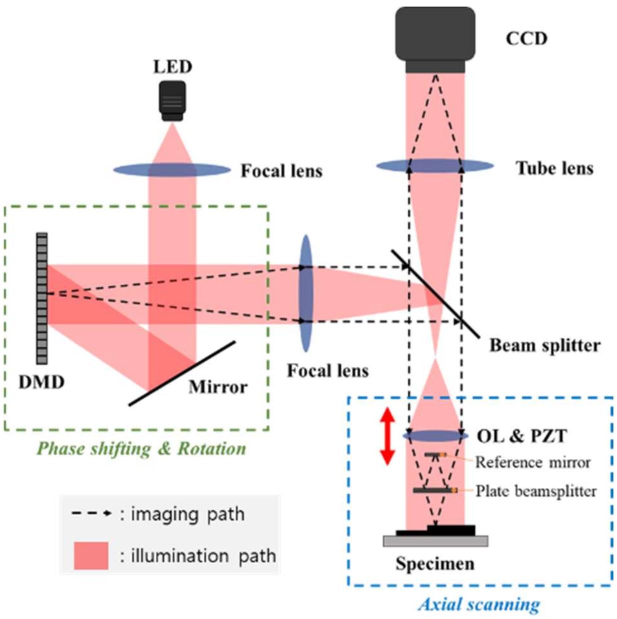

Figure 1. Optical configuration of HR-WLSI

At each axial position, high-resolution image of the generated various angle illumination pattern is obtained using 2D Fourier transform, and an interference signal graph (I) according to the scanning of the specimen is obtained as

$$I = [I_0(1 + V cos\phi)] \quad (1)$$

where I_0 is the light intensity, V is the envelope of the interference signal, and ϕ is the phase of the interference fringe. A high-resolution 3D image of the specimen is reconstructed by analyzing the interference signal graph (I) obtained through a white light scanning interferometry algorithm [8].

2.2 Lateral resolution enhancement principle

As shown in Fig. 2, lateral resolution can be improved through frequency synthesis of pattern images with phase shifted at various angles. Using phase shifted pattern images at three different rotation angles, three images are obtained for each rotation angle according to the phase shift. Representing these in the spatial frequency domain regions the following

$$\begin{aligned} D_{\theta,\phi_n}(k) = \frac{I_0}{2}[&S(k) \times H(k) \\ &+ \frac{1}{2} e^{-i\phi_n} S(k - k_\theta) \times H(k) \\ &+ \frac{1}{2} e^{i\phi_n} S(k + k_\theta) \times H(k)] \end{aligned} \quad (2)$$

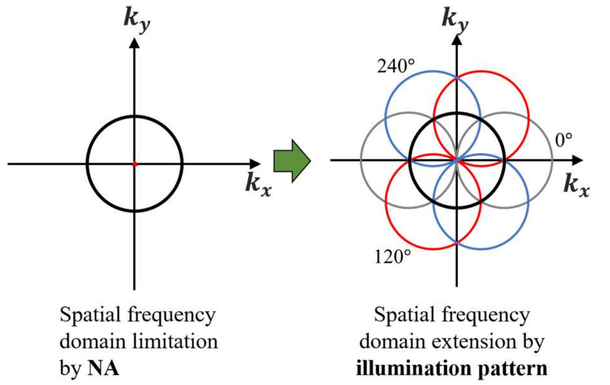

Figure 2. Extended spatial frequency region by SR-SIM

In Eq. (2), D_{θ,ϕ_n} represents the spatial frequency distribution of the phase shifted image at the rotation angle θ of the pattern, and $H(k)$ is the optical transfer function. Additionally, $S(k) \times H(k)$, $S(k - k_\theta) \times H(k)$, $S(k + k_\theta) \times H(k)$ denote the background noise and the spatial frequency distribution of the sample caused by the pattern in the spatial frequency domain. When the illumination pattern is phase-shifted with $\phi_{1,2,3}$=0, 2π/3 and 4π/3, these three components can be separately obtained with the following matrix operation.

$$\begin{bmatrix} S(k) \times H(k) \\ S(k - k_\theta) \times H(k) \\ S(k + k_\theta) \times H(k) \end{bmatrix} = \frac{2}{A} \begin{bmatrix} 2 & e^{-i0} & e^{i0} \\ 2 & e^{-i2\pi/3} & e^{i2\pi/3} \\ 2 & e^{-i4\pi/3} & e^{i4\pi/3} \end{bmatrix}^{-1} \begin{bmatrix} D_{\theta,0}(k) \\ D_{\theta,2\pi/3}(k) \\ D_{\theta,\pi/3}(k) \end{bmatrix} \quad (3)$$

As known in Eq. (3), there are three unknown parameters ($S(k) \times H(k)$, $S(k - k_\theta) \times H(k)$ and $S(k + k_\theta) \times H(k)$) with three phase-shifted measurement results at each rotation angle (ϕ_n) of the sinusoidal pattern, and then they can be calculated. In case of θ=0°, 120° and 240°, therefore, each set of $S(k) \times H(k)$, $S(k - k_\theta) \times H(k)$ and $S(k + k_\theta) \times H(k)$ is also obtained by using Eq. (3), and the extended whole spatial frequency content can be synthesized by the summation of all results with the aid of the Wiener filter to temper the discontinuity in the overlapped region. Subsequently, the synthesized spatial frequency region is broader than the original one limited by the NA of the objective lens as shown in Fig. 2, and the image reconstructed by the spatial frequency synthesis has higher lateral resolution than the original image [9].

3. Simulation results

Before the experiments, we performed simulations using a mosaic-patterned height sample. To replicate real experimental conditions, we generated 300 images containing interference signals and added angle-dependent phase-shifted pattern effects. Additionally, blur effects caused by scanning along the optical axis were incorporated into each image. The interference signals were analyzed using both the proposed method and the conventional WLSI algorithm [8,10] to perform a comparative verification.

The simulation parameters were set to central wavelength of 550 nm, NA of 0.1, magnification of 20x, and scanning step size of 50 nm. Figure 3 presents the reconstruction results and spatial frequency contents obtained using the proposed method compared to conventional WLSI. The expansion of the spatial frequency bandwidth enabled the retrieval of high-frequency components that were previously limited by the NA. Consequently, as demonstrated by the cross-sectional profile in Fig. 4, we confirmed that the period and height of the generated sample were precisely reconstructed.

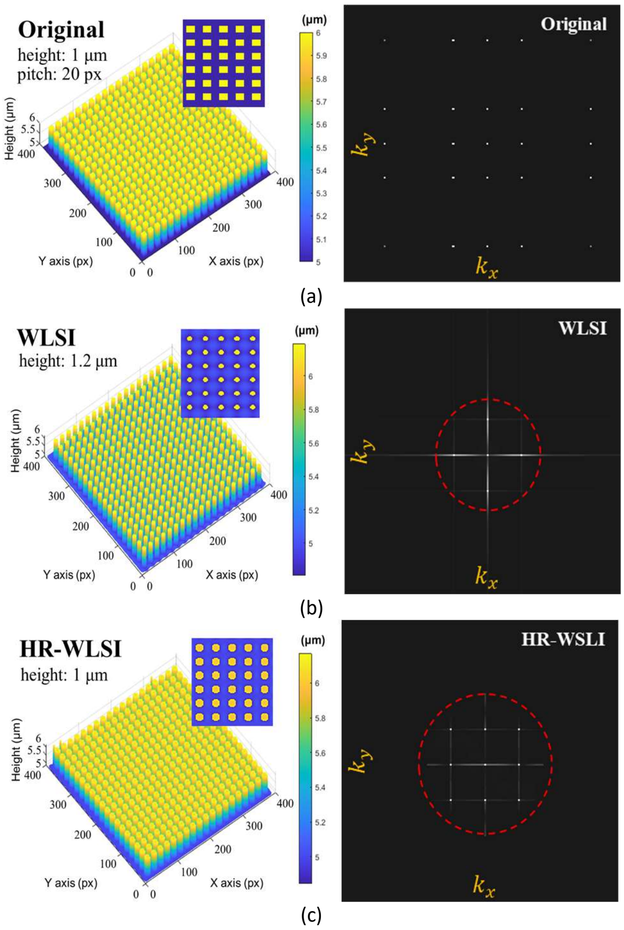

Figure 3. 3D surface profile and its spatial frequency content of (a) original specimen, (b) typical WLSI result and (c) HR-WLSI result

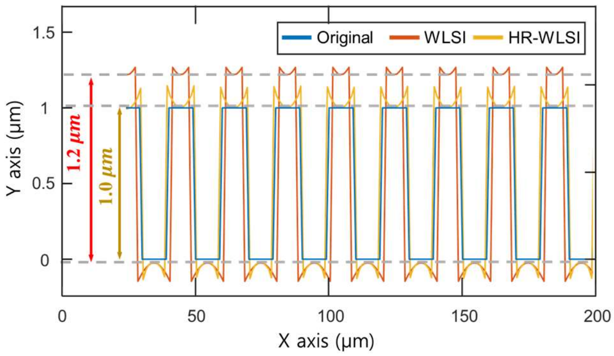

Figure 4. Cross-sectional spatial frequency content of resolution enhanced graph from the simulation of mosaic pattern

4. Experimental results

Based on the simulation results, specimen measurements were implemented. Figure 5 illustrates the measurement results of a defected plane mirror, confirming that scratches clearly appear using the proposed method compared to those by the conventional WLSI because of its better lateral resolution. In this setup, we observed that the spatial frequency region was expanded by a factor of approximately 1.44 as shown in Fig. 6.

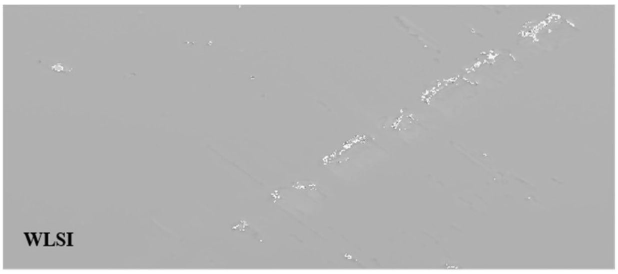

(a)

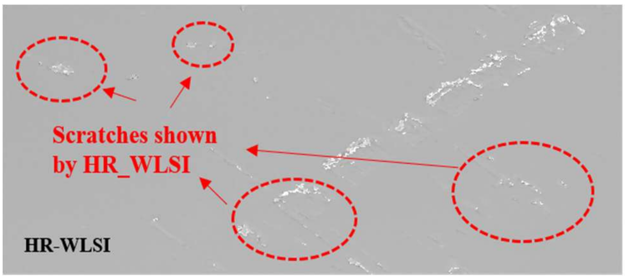

(b)

Figure 5. Mirror scratches obtained by (a) typical WLSI and (b) HR-WLSI

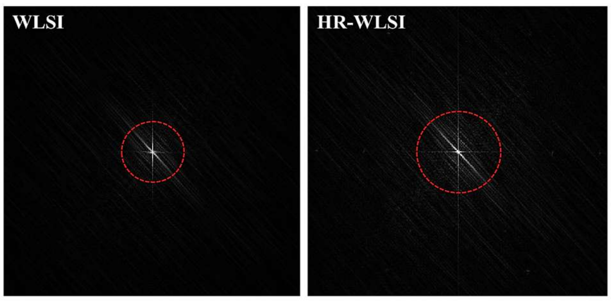

Figure 6. Spatial frequency content of defected plane mirror

Furthermore, as shown in Fig. 7 and Fig. 8, the measurement of a grating sample with a 3 μm pitch and 1 μm height yielded a height of 1.04 μm using the proposed method, whereas the WLSI method resulted in 1.48 μm. This confirms that the specimen height is reconstructed with greater precision due to the enhancement in lateral resolution.

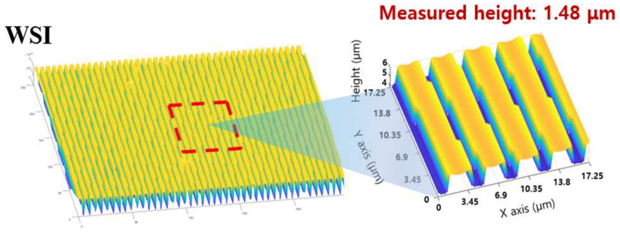

(a)

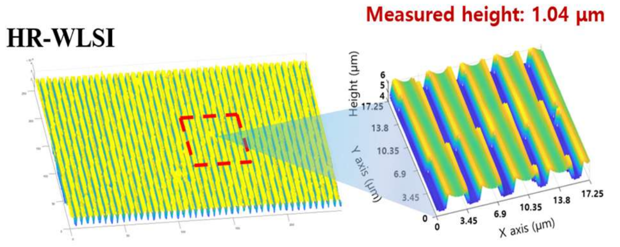

(b)

Figure 7. Reconstruction results of grating sample by (a) typical WLSI and (b) HR-WLSI

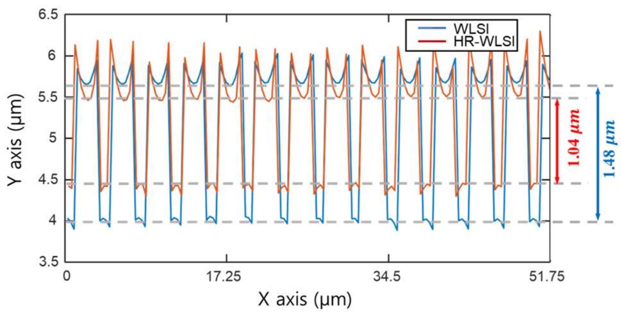

Figure 8. Cross-sectional result of grating sample

5. Conclusion

We demonstrated high resolution white light scanning interferometry by combining the operating principles of SIM and WLSI. In the experiments, the grating specimen was used to confirm the lateral resolution enhancement and 3D measurement capability, respectively. Additionally, we plan to conduct experiments to assess the uncertainty and precision of the results. We believe this combined system can be successfully applied in semiconductor and display industries.

References

[1] Kewei E, Li D, Yang L, Guo G, Li M, Wang X and Xiong Z 2017 Novel method for high accuracy figure measurement of optical flat Opt. Lasers Eng. **88** 162–166

[2] Schwider J and Falkenstoerfer O R 1995 Twyman-Green interferometer for testing microspheres Opt. Eng. **34** 2972-2975

[3] Nicolaus R A 1993 Precise method of determining systematic errors in phase-shifting interferometry on Fizeau interferences Appl. Opt. **32** 6380-6386

[4] Tay C J, Quan C and Shang H M 1998 Shape identification using phase shifting interferometry and liquid-crystal phase modulator Opt. Laser Technol. **30** 545–550

[5] Chen X, Zhong S, Hou Y, Cao R, Wang W, Li D, Dai Q, Kim D and Xi P 2023 Superresolution structured illumination microscopy reconstruction algorithms: a review Light Sci. Appl. **12** 172

[6] Gustafsson M G L 2005 Nonlinear structured-illumination microscopy: wide-field fluorescence imaging with theoretically unlimited resolution Proc. Natl. Acad. Sci. USA **102** 13081-13086

[7] Gustafsson M G L 2000 Surpassing the lateral resolution limit by a factor of two using structured illumination microscopy J. Microsc. **198** 82-87
[8] De Groot P and Deck L 1995 Surface profiling by analysis of white-light interferograms in the spatial frequency domain J. Mod. Opt. **42** 389-401
[9] Shroff S A, Fienup J R and Williams D R 2008 OTF compensation in structured illumination superresolution images Proc. SPIE **7094** 7-17
[10] De Groot P 2015 Principles of interference microscopy for the measurement of surface topography Adv. Opt. Photonics **7** 1-65